



Preparation of Fe³⁺-Deposited ZnS and its Photocatalytic Oxidation of Antibiotics Pollution

XIAOJIE ZHANG¹, YONGSHENG YAN^{2,*}, PENGWEI HUO² and ZIYANG LU²

¹Department of Chemistry and Biology, Suzhou University, Suzhou, P.R. China

²School of Chemistry and Chemical Engineering, Jiangsu University, Zhenjiang, P.R. China

*Corresponding author: Fax: +86 511 88791800; Tel: +86 511 88791800; E-mail: yys@ujs.edu.cn

(Received: 23 June 2011;

Accepted: 17 January 2012)

AJC-10985

The purpose of this paper is to prepare Fe³⁺-deposited ZnS and enhance the photocatalytic activity of ZnS under visible light irradiation. It is very significant to degrade ciprofloxacin using prepared photocatalyst by visible light irradiation. The bulk ZnS was synthesized by a simple hydrothermal method using Zn(CH₃COO)₂ and (NH₂)₂CS as main original reactant and poly(vinyl pyrrolidone) (PVP) (M = 10000) as the surfactant. The irradiation experiments were carried out in a photoreactor using two 150-W tungsten halogen lamps. The concentration of ciprofloxacin was determined spectrophotometrically. The efficiency of photocatalytic degradation of ciprofloxacin was affected by the amount of Fe³⁺ ions on the surface of ZnS, irradiation time and the dosage of photocatalyst. The kinetics data were fit Langmuir-Hinshelwood kinetic expression. The proposed mechanism could explain the processes of photocatalytic degradation of ciprofloxacin, as fluoroquinolones pollution, could be degraded using Fe³⁺-deposited ZnS as photocatalyst under visible irradiation. The prepared catalysts were characterized by SEM, XRD and diffusive reflectance spectra. Photodegradation of ciprofloxacin follows the first-order kinetics and the degradation rate is 0.042 min⁻¹ at 20 mg L⁻¹ initial concentration of ciprofloxacin.

Key Words: ZnS, Fe³⁺-Deposit, Visible light irradiation, Photocatalytic, Degradation, Ciprofloxacin, Fluoroquinolones.

INTRODUCTION

Polluted water has posed a serious problem to the environment. Besides water pollutants such as pesticides, dyes, surfactants and pharmaceuticals are an emerging group of aquatic contaminants. Fluoroquinolones (FQs) are a class of potent synthetic antibiotics that are widely used in agriculture, veterinary medicines and human prescription. Several recent studies have reported the spread presence and potential toxicities of fluoroquinolones¹⁻³ in many countries such as Switzerland, the United States, Australia and China, which is necessitate to understand their environmental fate and to avoid their risks. At present, most of the wastewater treatment plants (biodegradation and adsorption) are not designed to completely remove most pharmaceuticals and consequently these compounds are released into environmental aquatic bodies.

Ciprofloxacin (Fig. 1), one of the most frequently prescribed human-use fluoroquinolones in many countries. Similar to many pharmaceutical compounds, ciprofloxacin is a fluoroquinolone group broad-spectrum antibiotic agent and poor biodegradable, making physical-chemical technologies indispensable for its degradation prior to discharge in the environment⁴⁻⁶.

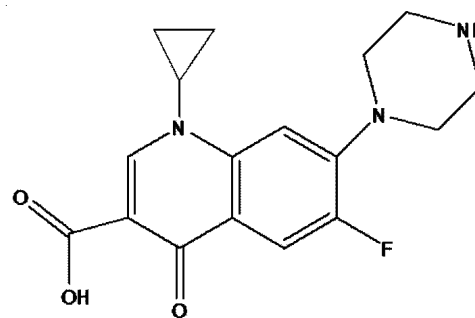


Fig. 1. Structure of ciprofloxacin

Advanced oxidation processes characterized by the generation of hydroxyl radicals at ambient conditions, which are known as an effective method to remove not or hard biodegradable organic pollutants from environmental wastewater (ground-, surface- and wastewater)⁷⁻⁹. Their effectiveness results from the fact that the *in situ* generated hydroxyl radicals are highly reactive species, able to oxidize organic molecules. The radicals are produced by combinations of ozone, hydrogen peroxide, UV radiation, ferrous ions and titanium dioxide. Numerous authors investigated the degradation of organic pollutants such as pesticides, dyes, pharmaceuticals, aromatic

compounds, nitrophenols or surfactants by photo-fenton oxidation¹⁰⁻¹³.

Titania (TiO₂) was first founded to be photoassisted electrochemical splitting of water since 1972 by Fujishima, semiconductor photocatalysts have attracted considerable attention in the fields of catalysis, electrochemistry and photochemistry in recent years. That can be attributed to their significant effects on solving environmental problems, such as air or water pollution^{14,15}. Among different semiconductors, zinc sulfide (ZnS) is an important one with a large exciton binding energy (E_g) (40 meV) and a small Bohr radius (2.4 nm), which has been considered to be a promising material for ultraviolet-light emitting diodes, infrared windows and photocatalysts. In recent years, many researchers reported the preparation of one-dimensional ZnS nanostructures including nanorods, nanotubes, nanobelts and nanowires, *etc.* There are many methods reported on the preparation of one-dimensional nanostructures of ZnS¹⁶⁻¹⁸. ZnS is II-VI group compound semiconductor, which is an important material with the band gap energy (E_g) of 3.6 eV. It has been extensively studied for a variety of applications in the field of optics, electronics, photocatalysis, *etc.* It is known that transition metal ions doped into catalysts can increase the quantum efficiency of the heterogeneous photocatalytic property by acting as electron (or hole) traps and by changing the e⁻/h⁺ pair recombination rate¹⁹⁻²⁴. So, in this work, Fe³⁺ ions of different concentrations were added into the prepared ZnS. The objective of this research is to investigate the effect of transition metal ions on the photocatalytic activity of degradation efficiency. Photocatalytic activity of it was evaluated by degrading ciprofloxacin as a model organic compound.

EXPERIMENTAL

All chemicals used throughout the study were of analytical grade and their solutions were prepared in distilled water. ciprofloxacin (Shanghai Institute of Biological Products, Shanghai, China), Fe(NO₃)₃, Zn(CH₃COO)₂, CS(NH₂)₂, NaOH (Sinopharm Chemical Reagent. CO. Ltd., Shanghai, China), PVP (Aladdin reagent, Shanghai, China).

JSM-7001 field emission scanning electron microscope (Hitachi, Japan), X-ray diffraction (XRD) (Siemens, Germany), UV-2450 spectrophotometer (Shimadzu, Japan).

Photocatalysts preparation: At first, Zn(CH₃COO)₂ (6 mmol) was dissolved in 10 mL deionized water, then the NaOH solution (3.0 mol L⁻¹) was added drop-wise to the Zn(CH₃COO)₂ aqueous solution until the pH is about 10 and the milky white emulsion formed. After stirring for 10 min, poly(vinyl pyrrolidone) (0.05 g) was added into the above mixture under continuous stirring for 10 min. And then thiourea (12 mmol) was introduced to the above solution under stirring for another 10 min. Then the mixed solution was transferred into a Teflon-lined stainless-steel autoclave of 30 mL capacity. The Teflon-lined autoclave was sealed tightly and maintained at 160 °C for 48 h and then cooled to room temperature. The white product obtained was separated by centrifugation and repeatedly washed with deionized water and ethanol for several times to remove impurities. Finally the sample was dried in a vacuum at 55 °C for 12 h.

Doping was performed by impregnation of ZnS with aqueous solutions of Fe(NO₃)₃ by an incipient wetness impregnation method at 298 K as follows. The mixture (ZnS and Fe precursor) was stirred during 24 h. Later, water was evaporated by heating 393 K during 12 h. Finally, the catalysts were dried at 358 K and set aside. According to the concentrations of Fe precursor, the prepared catalysts were labeled as 2, 4, 6 and 8 wt. %, respectively.

Characterization: JSM-7001 field emission scanning electron microscope (SEM) was used for the determination of the surface and size of the catalysts. X-Ray diffraction (XRD) patterns were used with Cu K_α radiation (λ = 0.1541 nm). The phase structures were determined by X-ray diffractometer using graphite monochromatic copper radiation (Cu K) at 40 kV, 30 mA over the 2θ range 10-80°. The 2θ scanning angle range was 10-80° with a step of 0.1° s⁻¹. Diffusive reflectance UV-VIS (DRS) adsorption spectra were recorded on an UV-2450 spectrophotometer (Japan).

Photocatalytic reaction: The photocatalytic activity of the prepared photocatalysts was evaluated by the photocatalytic oxidation degradation of ciprofloxacin. Two tungsten halogen lamps (LZG 220/240-150, R7S) were used as the mock visible light source at a 12 cm separation distance. The reaction system was maintained at ambient temperature. In a typical experiment, aqueous solution of ciprofloxacin (100 mL, 20 mg L⁻¹) and the different amount of catalysts were added into the solution in the beaker with a magnetic stirrer. Prior to light irradiation, the suspension was kept still in the dark to ensure the establishment of an adsorption/desorption equilibrium. The suspension was kept under constant air equilibrated condition. At the intervals of given irradiation time, 5 mL of the suspension was collected and centrifuged for 20 min (3000 rpm) to remove the particles. The ciprofloxacin concentration was determined by measuring the UV-VIS absorbance of the aqueous solution of ciprofloxacin at maximum wavelength (278 nm).

RESULTS AND DISCUSSION

XRD analysis: The prepared ZnS samples were analyzed for their phase composition and microstructure by XRD. The

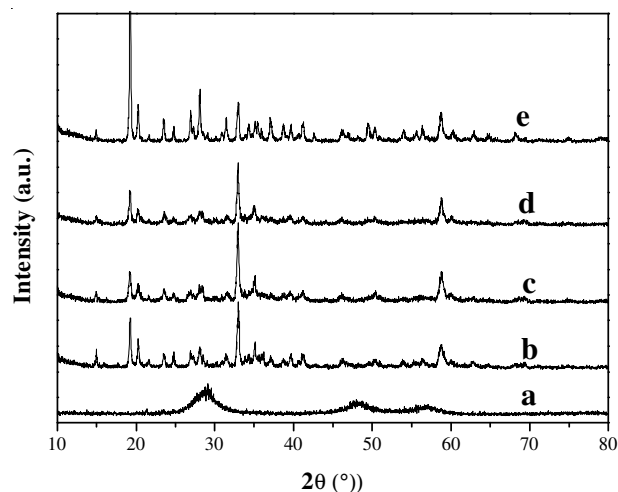


Fig. 2. XRD pattern of the prepared ZnS samples, a, b, c, d and e response the bulk ZnS, 2, 4, 6 and 8 % Fe-deposited ZnS, respectively

diffraction peaks of bulk ZnS can be indexed to a pure cubic phase, which is in good agreement with the standard values for the bulk cubic ZnS (JCPDS: 36-1460). No other peaks or impurities have been detected indicating the high purity of the product. The diameter of the prepared ZnS is 150 nm by Scherrer formula. When the other patterns were compared with the bulk ZnS, it was found that 2 θ degrees peaks observed at 19.16, 32.96, 35.04 and 58.82° for Fe-deposited ZnS. In addition, the peaks of the bulk ZnS at 29.2, 48.34 and 56.96° become weaker in the process of deposit Fe³⁺ ions. However, the values of these peaks will not change. These results support that the current doping method do not modify the structure of ZnS.

Morphology: The size and morphology of the synthesized products were observed by FESEM. The size of the ZnS is about 3 μ m, the possible reason is the size effect of the microscopic particles. Fig. 3 shows the SEM image of bulk ZnS and 6 wt. % Fe³⁺-deposited ZnS. After depositing Fe³⁺, the surface of ZnS become unshaped, adding the surface area of ZnS. That can supply more activity sites on the surface of deposited ZnS. Thus, these sites could enhance the photocatalytic activity of Fe³⁺-deposited ZnS.

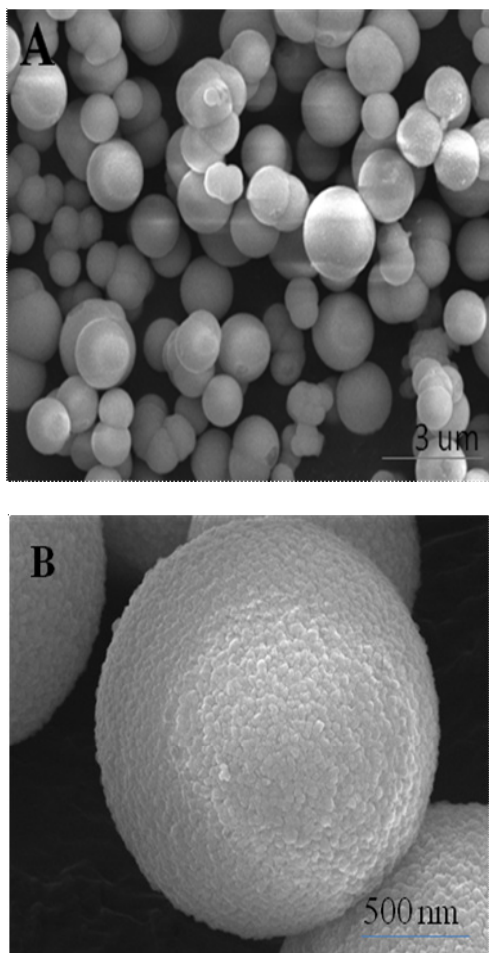


Fig. 3. SEM of bulk ZnS (A) and 6 wt. % Fe³⁺-deposited ZnS (B)

Diffusive reflectance spectra: To investigate the optical properties of the obtained ZnS micro/nano-crystals, the room temperature UV-VIS absorption spectra of the solid powder

was recorded (Fig. 4). Compared with that of the bulk ZnS, the absorption spectra of the ZnS samples exhibited a blue shift, indicating that the ZnS were quantum-confined. Such quantum-confined effect gives rise to high negative reduction potential of the electrons. Therefore, the deposited ZnS are expected to have high photocatalytic activities.

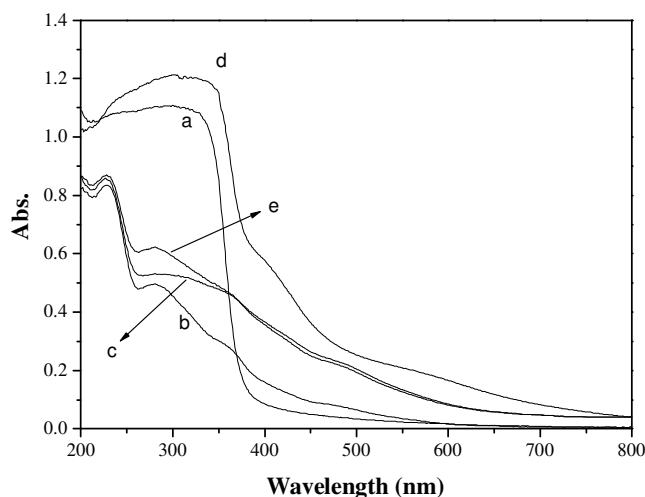


Fig. 4. Diffusive reflectance spectra of different catalysts samples, a, b, c and d response bulk ZnS, 2, 4, 6 and 8 wt. % Fe-deposited ZnS, respectively

Diffuse reflectance spectra (DRS) technique is a useful technique to characterize the optical absorption properties of nanoparticles. The DRS spectra of Fe-deposited ZnS with different modification level in comparison with bulk ZnS are shown in Fig. 4. For bulk ZnS, an absorption edge at UV below 300 nm (since the band-gap of ZnS is about 3.6 eV). The bulk ZnS has no absorption in visible region (> 400 nm), whereas Fe-deposited ZnS samples exhibit red-shifts to the edge of light absorption at 400-600 nm. The light absorption in the range extends from 450-600 nm with increasing Fe³⁺ content in ZnS.

From Fig. 4, it is observed that 6 wt. % Fe ZnS samples with low iron content shows a constant absorption in the visible region which is higher than bulk ZnS. It can also be noticed that Fe deposited ZnS particles have enhanced absorption characteristics in region of 400-550 nm and this enhancement increases as the deposited Fe is increased, accompanying with the change of particles colour from white to yellow and dark cream. Compared the curves of Fig. 2a-b, it seems that adsorption of light under visible light depends on the addition of Fe.

Photocatalytic degradation of ciprofloxacin: To test for the photocatalytic degradation of ciprofloxacin by bulk ZnS and deposited-ZnS nano-(micro) particles, a solution containing ciprofloxacin and prepared catalysts particles is photoirradiated under visible light. And the processes of the experiments were according to the experimental section. The photocatalytic degradation efficiencies were calculated using the following equation (eqn. 1):

$$E (\%) = \frac{A_0 - A_t}{A_0} \times 100 \quad (1)$$

where A_0 and A_t are the absorbance of ciprofloxacin before and after irradiation (t min). The results show of different catalysts irradiation under visible light (Fig. 5a). From the Fig. 5a, it indicates the degradation efficiency is very low in the presence of bulk ZnS (only 47.4 %). It was observed that photocatalytic performance of Fe-deposited ZnS for degradation of ciprofloxacin is higher than that of bulk ZnS under visible light. The 6 wt. % Fe-deposited ZnS exhibit the maximum catalytic efficiency (98.85 %) after 1 h irradiation. The effect of Fe^{3+} doping on the photocatalytic activity under visible light irradiation should be due to the reason that an appropriate amount of Fe^{3+} ions can act as intermediates for photo-generated holes and electrons transfer and inhibit the recombination of holes and electrons. However, when the amount of Fe^{3+} ions becomes too large, Fe^{3+} ions can act as the recombination centers for the photo-generated electrons and holes, resulting in the decrease of photocatalytic activity. Thus, this catalyst can be used after the experiments.

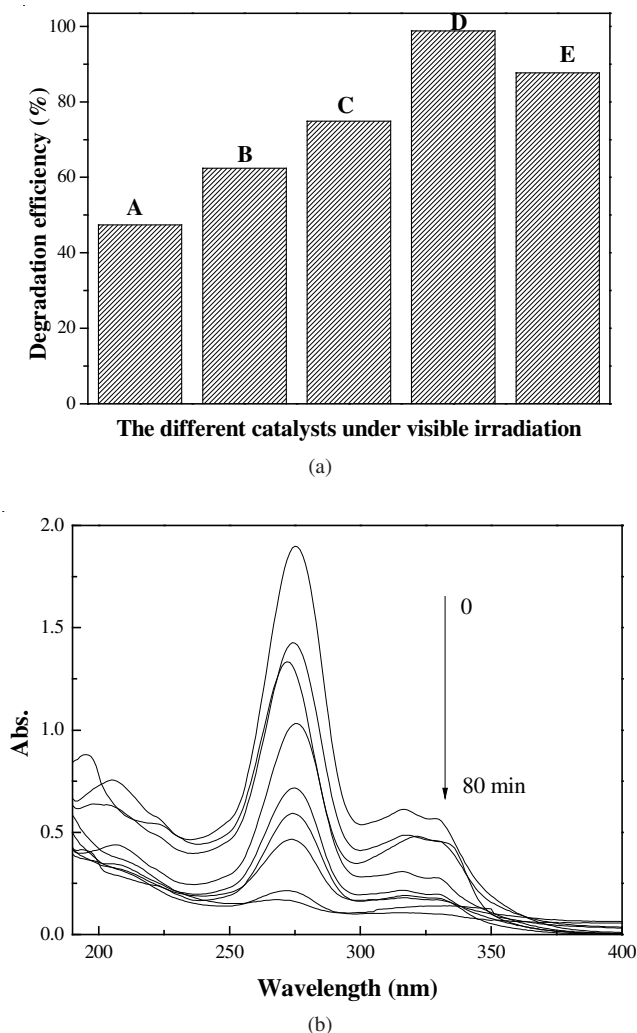


Fig. 5. (a) Different catalysts on the degradation ciprofloxacin under visible light irradiation (A, B, C, D response the bulk ZnS, 2, 4, 6 and 8 wt. %, respectively). (b) UV-VIS absorption spectra of ciprofloxacin during the photocatalytic degradation with different irradiation times

Fig. 5b shows the spectral changes of ciprofloxacin in the presence of 6 wt. % Fe-deposited-ZnS under visible irradiation. The maximum absorbance of ciprofloxacin at 273 nm greatly

decreases with the increase of irradiation time. At the irradiation time of 1 h, the absorbance dropped rapidly from 1.98 to the initial 0.05 and the degradation efficiency was calculated close to 100 %. As a comparison, we studied the direct photodegradation of ciprofloxacin without deposited-ZnS under the same conditions. The results prove that the deposited-ZnS exhibit strong photocatalytic activity and photocatalytic efficiency towards ciprofloxacin. The new absorption band appeared in the ultraviolet region, indicating that inorganic ions were created in the process of the degradation since their absorption would appear this area.

Effect of initial ciprofloxacin concentration: Since the pollutant initial concentration is an important parameter in the treatment, the effect of initial ciprofloxacin concentrations on photocatalytic degradation rate was investigated over the concentration range of 10-50 mg L^{-1} of ciprofloxacin (Fig. 6). The results show that the degradation rate decreases as the initial ciprofloxacin concentration increases. This is due to the reason that the matter when the amount of ciprofloxacin over the maximum of catalyst could be degraded.

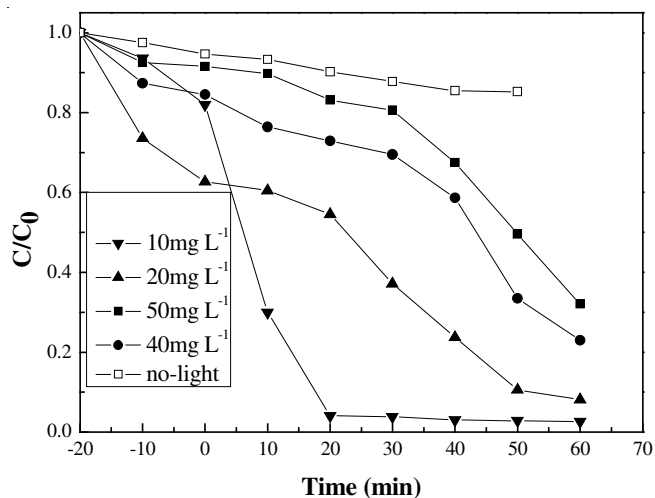


Fig. 6. Effect of initial concentration on degradation efficiency

The Langmuir-Hinshelwood kinetic expression^{16,24} has been used for heterogeneous photocatalysis to describe the relationship between the initial degradation rate and the initial concentration. In this model, the reaction rate for second-order surface decomposition of ciprofloxacin (CPLX) is written as follows:

$$\text{Rate} = -\frac{dC}{dt} = k_c \frac{K_{\text{CPLX}}C}{1 + K_{\text{CPLX}}C_0} = k_c K \quad (2)$$

$$K = \frac{K_{\text{CPLX}}C}{1 + K_{\text{CPLX}}C_0} \quad (3)$$

where C is the ciprofloxacin concentration at time t , k_c is the second-order rate constant, $K_{\text{ciprofloxacin}}$ is the equilibrium adsorption constants of ciprofloxacin onto Fe-deposited ZnS and C_0 is the initial concentration of ciprofloxacin. According to the above equation, the photocatalytic degradation of ciprofloxacin in the presence of Fe-deposited ZnS exhibits pseudo first-order kinetics with respect to ciprofloxacin concentration as in eqn. 4

$$-\frac{dC}{dt} = k_{\text{obs}}C = k_c \frac{K_{\text{CPLX}}}{1 + K_{\text{CPLX}}C_0} C \quad (4)$$

where k_{obs} is the observed pseudo-first-order rate constant for the photocatalytic oxidation of ciprofloxacin. Therefore, the integration of eqn. 4 results in

$$\ln \frac{C_0}{C} = k_{\text{obs}} t \quad (5)$$

Based on eqn. 5, the straight line relationship of $\ln(C_0/C)$ versus irradiation time was observed as indicated in Fig. 7 and Table-1.

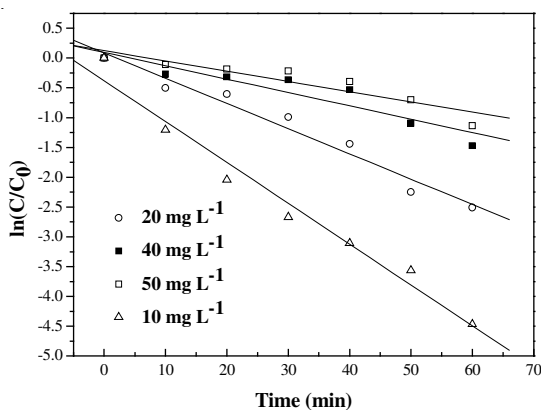


Fig. 7. Plot of $\ln(C/C_0)$ versus irradiation at different initial ciprofloxacin concentration

The relationship between k_{obs} and C_0 from eqn. 4 can be expressed as eqn. 6

$$\frac{1}{k_{\text{obs}}} = \frac{1}{k_c K_{\text{CPLX}}} + \frac{C_0}{k_c} \quad (6)$$

Eqn. 6 shows that the linear expression can also be obtained by plotting the reciprocal of degradation rate ($1/k_{\text{obs}}$) as a function of the initial ciprofloxacin concentration. Based on this equation, the values of k_{obs} at different initial ciprofloxacin concentration were fitted and the plotted in Fig. 8. By means of a least square best fitting procedure, the values of the adsorption equilibrium constant ($K_{\text{ciprofloxacin}}$) and the second-order rate constant (k_c) were obtained and this value found to be $K_{\text{ciprofloxacin}} = 0.3765 \text{ L mg}^{-1}$ and $k_c = 0.926 \text{ mg L}^{-1} \text{ min}^{-1}$ ($R^2 = 0.998$), respectively.

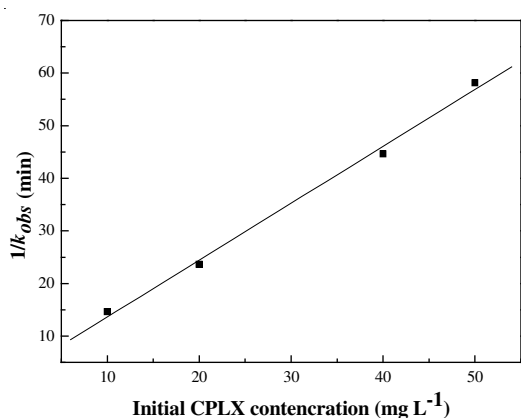


Fig. 8. Plot of the initial ciprofloxacin (CPLX) concentration versus the reciprocal of the observed first-order rate constant ($1/k_{\text{obs}}$)

Effect of the photocatalysts dosage on degradation efficiency:

The dosage of catalyst plays an important role in catalytic oxidation reactions during the processing of industry organic pollutants. Accordingly, the effect of the dosage of prepared catalyst on ciprofloxacin degradation was evaluated (Fig. 9). Fig. 9 shows that the concentration of ciprofloxacin can increase in the absence of 6 wt. % Fe-deposited-ZnS. The results revealed that the greatest degradation efficiency was achieved when the amount of catalyst increased 1.5 g L^{-1} . However, when the amount exceeds this value, the removal efficiency declines on the contrary. The reason may be due to more catalysts effect the absorbance of the effective photons (mainly ultraviolet rays) and reduce the activity of the photocatalyst. Therefore, this value (1.5 g L^{-1}) was taken to be the optimum dosage of the catalyst.

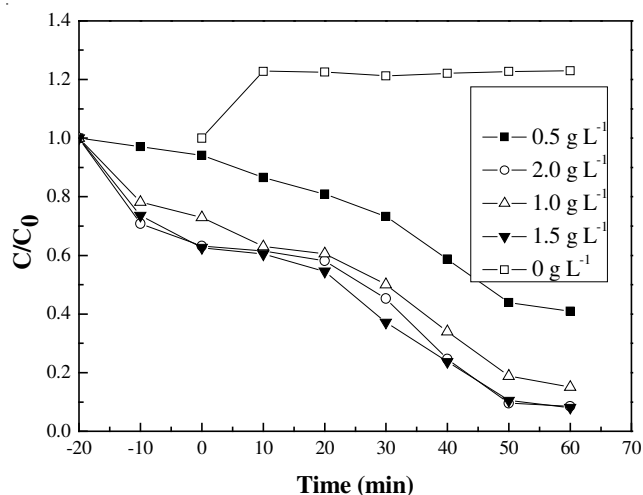


Fig. 9. Effect of the catalysts dosage on degradation efficiency

Possible mechanism for ciprofloxacin degradation under visible light:

Photodegradation of ciprofloxacin is initiated by photoexcitation in the presence of the Fe³⁺-deposited ZnS. Fig. 10 shows the scheme of the photocatalytic degradation ciprofloxacin under visible light. Light-induced electrons/holes pair formation in the surface of semiconductor particles. Fe³⁺ ions acting as both electrons and holes traps, can turn into Fe²⁺ and Fe⁴⁺ ions by trapping photogenerated electrons and holes traps, respectively (eqns. 7-10), accompanied by subsequent interfacial electron (hole) transfer, has always been considered as the first step of the photocatalytic action of semiconductor particles. Fe²⁺ ions can be oxidized to Fe³⁺ ions by transferring electrons to absorbed O₂ on the surface of ZnS (eqn. 10). Meanwhile, the adsorbed O₂ is reduced to O₂⁻, which can further degrade ciprofloxacin. Similarly, Fe⁴⁺ ions also are reduced to Fe³⁺ ions by releasing electrons, which surface hydroxyl group translates into hydroxyl radical ·OH eqn. 11. The high oxidative potential of holes can lead to direct and indirect oxidation of ciprofloxacin. As a result, the introduction of appropriate Fe³⁺ ions is responsible for the reduction of the photogenerated hole-electron recombination rate and favours the improvement of photocatalytic activity. After ciprofloxacin was degradation, the active sites left on the surface of catalyst and the conditions provided for adsorption ciprofloxacin again, then degradation and again. The proposed mechanism for

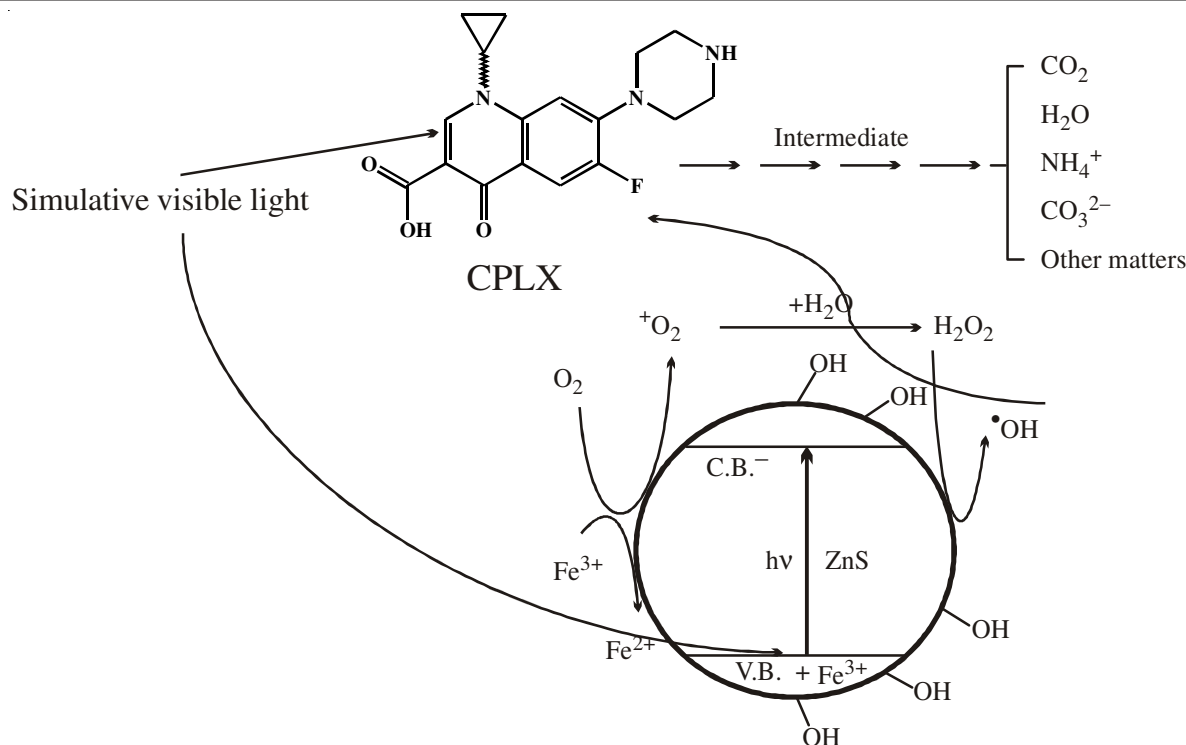
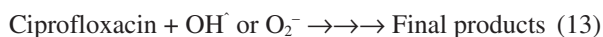
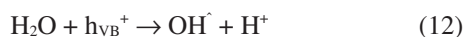
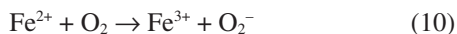


Fig. 10. Scheme of photocatalytic degradation of ciprofloxacin

ciprofloxacin degradation using photocatalysts (Fe^{3+} -deposited ZnS) was suggested as follows:



Reuseability: The reuseability of the Fe-deposited ZnS catalyst was tested by repeating the photoreduction degradation experiments under the same conditions using the recycled catalyst. The catalytic activity of Fe^{3+} -deposited ZnS loss was not considerable after used five times. The highly catalytic activity of ZnS probably results from their microstructures.

Conclusion

ZnS micro/nano-crystals were synthesized *via* hydrothermal method using PVP as the surfactant. The obtained Fe^{3+} -deposited ZnS micro/nanocrystals are about 3 μm with narrow size distribution and show good photocatalytic activity for degradation of ciprofloxacin.

ACKNOWLEDGEMENTS

The authros gratefully acknowledge the financial support of the Research Foundation of Jiangsu University, China (No. 04JDG017) and the Graduate Innovation Project of Jiangsu Province (CX09B_208z).

REFERENCES

1. T. Paul, P.L. Miller and T.J. Strathmann, *Environ. Sci. Technol.*, **41**, 4720 (2007).
2. B. Dewitte, J. Dewulf, K. Demeestere, V.V.D. Vyvere, P.D. Wispelaere and H.V. Langenhove, *Environ. Sci. Technol.*, **42**, 4889 (2008).
3. H. Zhang and C. Huang, *Chemosphere*, **66**, 1502 (2007).
4. E. Guinea, J.A. Garrido, R.M. Rodríguez, P.-L. Cabot, C. Arias, F. Centellas and E. Brillas, *Electrochim. Acta*, **55**, 2101 (2010).
5. R.J. Carman, M.A. Simon, H. Fernandez, M.A. Miller and M.J. Bartholomew, *Regul. Toxicol. Pharmacol.*, **40**, 319 (2004).
6. P. Tau and T. Nyokong, *J. Mol. Catal. A: Chem.*, **273**, 149 (2007).
7. J. Liu, B. Geng and S. Wang, *Crystal Growth Design*, **9**, 4384 (2009).
8. A.G.S. Prado and L.L. Costa, *J. Hazard. Mater.*, **169**, 297 (2009).
9. T. Oncescu, M.I. Stefan and P. Oancea, *Environ. Sci. Pollut. Res.*, **17**, 1158 (2010).
10. L.L. Costa and A.G.S. Prado, *J. Photochem. Photobiol. A: Chem.*, **201**, 45 (2009).
11. I. Liu, L. Lawton and P.K.J. Robertson, *Environ. Sci. Technol.*, **37**, 3214 (2003).
12. M.A. Fox and M.T. Dulay, *Chem. Rev.*, **93**, 341 (1993).
13. X. Jiang and T. Wang, *Environ. Sci. Technol.*, **41**, 4441 (2007).
14. N. Klammer, N. Miranda, S. Malato, A. Agüera, A.R. Fernández-Alba, M.I. Maldonado and J.M. Coronado, *Catal. Today*, **144**, 124 (2009).
15. C. Wang, Y. Ao, P. Wang, S. Zhang, J. Qian and J. Hou, *Appl. Surf. Sci.*, **256**, 4125 (2010).
16. S. Feng, J. Zhao and Z. Zhu, *Mater. Sci. Eng. B*, **150**, 116 (2008).
17. A. Franco, M.C. Neves, M.M.L. Ribeiro Carrott, M.H. Mendonca, M.I. Pereira and O.C. Monteiro, *J. Hazard. Mater.*, **161**, 545 (2009).
18. M. Asiltrük, F. Sayilkan and E. Arpaç, *J. Photochem. Photobiol. A: Chem.*, **203**, 64 (2009).
19. K. Naeem and F. Ouyang, *Phys. B*, **405**, 221 (2010).
20. J. Arana, O.G. Díaz, M.M. Saracho and J.M.D. Rodríguez, *Appl. Catal. B: Environ.*, **32**, 49 (2001).
21. B. Xin, Z. Ren, P. Wang, J. Liu, L. Jing and H. Fu, *Appl. Surf. Sci.*, **253**, 4390 (2007).
22. P. Yang, C. Lu, N. Hua and Y. Du, *Mater. Lett.*, **57**, 794 (2002).
23. T. Ohno, Z. Miyamoto, K. Nishijima, H. Kanemitsu and F. Xueyuan, *Appl. Catal. A: Gen.*, **302**, 62 (2006).
24. H.-S. Son, S.-J. Lee, I.-H. Cho and K.-D. Zoh, *Chemosphere*, **57**, 3 (2004).